

A cortical neuropeptide with neuronal depressant and sleep-modulating properties

Luis de Lecea*, José R. Criado†, Óscar Prospero-García†, Kaare M. Gautvik*, Paul Schweitzer†, Patria E. Danielson*, Charles L. M. Dunlop*, George R. Siggins†, Steven J. Henriksen† & J. Gregor Sutcliffe*

Departments of * Molecular Biology and † Neuropharmacology, The Scripps Research Institute, La Jolla, California 92037, USA

ACETYLCHOLINE (ACh) plays a key role in the transitions between the different phases of sleep¹: Slow-wave sleep requires low ACh concentrations in the brain, whereas rapid-eye-movement (REM) sleep is associated with high levels of ACh. Also, these phases of sleep are differentially sensitive to a number of endogenous neuropeptides and cytokines, including somatostatin, which has been shown to increase REM sleep without significantly affecting other phases². Here we report the cloning and initial characterization of cortistatin, a neuropeptide that exhibits strong structural similarity to somatostatin, although it is the product of a different gene. Administration of cortistatin depresses neuronal electrical activity but, unlike somatostatin, induces low-frequency waves in the cerebral cortex and antagonizes the effects of acetylcholine on hippocampal and cortical measures of excitability. This suggests a mechanism for cortical synchronization related to sleep.

While characterizing region-specific brain messenger RNAs, we isolated a complementary DNA clone whose sequence suggested that it corresponded to an mRNA that encoded a new protein of 112 amino-acid residues which we called preprocortistatin. Alignment of preprocortistatin with the 116-residue sequence of preprosomatostatin (Fig. 1) revealed several points of structural similarity, although the only extended amino-acid identity was at their carboxy termini. Preprocortistatin starts with a 27-residue apparent secretion-signal sequence. Cleavage of the preprospecies to procortistatin would produce a protein that could be proteolytically matured further at either of two tandem basic amino-acid pairs to produce cortistatin-29 and cortistatin-14, analogous to the cleavage of preprosomatostatin at 28 and 14 residues³, or at both basic pairs to produce cortistatin-13 as well. Cortistatin-13 is unrelated to any known species, whereas cortistatin-14 shares 11 of 14 residues with somatostatin-14, including two cysteines that may cause the peptide to cyclize, and the FWKT sequence that is critical for somatostatin binding to its receptors⁴. Cortistatin-14 and somatostatin-14 are permuted by one amino acid (the alignment of cortistatin begins at residue 2 of somatostatin; cortistatin terminates with a lysine that extends one residue beyond the C-terminal cysteine of somatostatin) (Fig. 1). This difference and their cDNA sequences indicate clearly that they are the products of separate genes.

FIG. 1 Predicted amino-acid sequence of preprocortistatin. Preprocortistatin's deduced amino-acid sequence begins with a putative secretion signal peptide, whose predicted cleavage site is indicated by an arrow. The only region of extended similarity between cortistatin and somatostatin lies in the C terminus. Alignment of cortistatin-29 (CST) and somatostatin-28 (SST) amino-acid sequences shows that both statins share the critical residues for binding to the receptors and the cysteines that are likely to render the peptides cyclic. The basic amino acids that are putative processing sites are boxed. Sequence alignment was performed with the BESTFIT program (GCG group, University of Wisconsin).

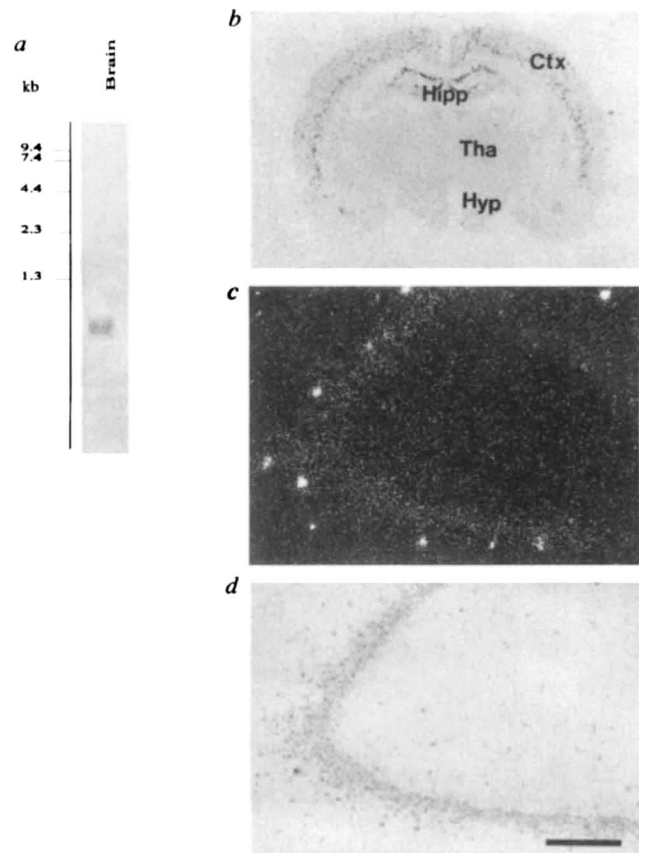
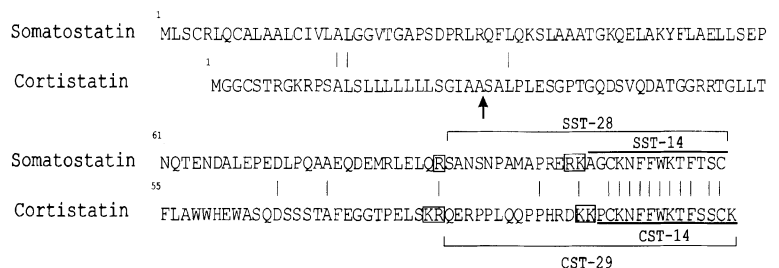


FIG. 2 Cortistatin is brain-specific. *a*, Northern blot containing 2 µg poly(A)-selected RNA from rat brain. *b*, *In situ* hybridization autoradiograph showing a coronal section of a rat brain hybridized with a cortistatin riboprobe. Note that the signal is restricted to individual sparse cells in the cortex and hippocampus. No signals were detected in the hypothalamus, a physiologically important site of somatostatin expression. In the hippocampal formation, cortistatin expression was restricted to scattered non-pyramidal cells in the subiculum and stratum oriens of CA1 and CA3 (*c*; *d* is the brightfield image of *c*; scale bar, 200 µm). *In situ* hybridization was done on free-floating sections as described¹⁸.

We determined the distribution of preprocortistatin mRNA by northern blotting. A single band of ~600 nucleotides was detected in samples prepared from brain (Fig. 2a), but not from adrenal gland, liver, spleen, thymus, ovary, testes or anterior pituitary (results not shown). We then examined the cellular distribution of cortistatin mRNA by *in situ* hybridization on rat brain sections. Signals were detected only in scattered cells throughout the cerebral cortex and hippocampus (Fig. 2b), but not in hypothalamus, an important site of somatostatin expression. In the hippocampus, we found cortistatin mRNA expression in some non-pyramidal cells in the subiculum and in the stratum oriens of the CA1 and CA3 fields, suggesting that cortistatin

mRNA might be present in GABAergic interneurons (Fig. 2c, d). We therefore performed double *in situ* hybridization experiments to detect co-expression of cortistatin and GAD₆₅/GAD₆₇ mRNAs, which encode the enzymes involved in GABA synthesis⁵. All cortistatin-expressing cells also contained either GAD₆₅ or GAD₆₇ mRNA, which was evidence for the GABAergic nature of these neurons (not shown).

We examined the binding of chemically synthesized, cortistatin-14 peptide to somatostatin receptors on GH₄ pituitary cells. Both cortistatin-14 and somatostatin-14 effectively displaced bound [¹²⁵I]-labelled somatostatin-14 in a dose-dependent manner with estimated K_ds (5 × 10⁻⁹ M; Fig. 3a) very close to that previously reported for somatostatin⁶. To investigate whether cortistatin regulates activation of the somatostatin receptor, we determined the concentration of cyclic AMP following stimulation of GH₄ cells with vasoactive intestinal peptide (VIP) or thyroid-releasing hormone (TRH) in the presence or absence of either cortistatin or somatostatin. Both statin peptides effectively inhibited stimulation by VIP and TRH (Fig. 3c). Cortistatin or somatostatin alone had no effect on basal cAMP concentrations (Fig. 3b). Both peptides at 10⁻⁸ M completely inhibited TRH, but attenuated the effect of VIP in a dose-dependent manner by ~50% at 10⁻⁶ M. Cortistatin therefore appears to act as an agonist on the endogenous somatostatin receptors expressed by GH₄ cells, although these cells may express a heterogeneous population of receptors and the agonist activity may not necessarily be its function at its sites of expression.

We tested whether cortistatin had somatostatin-like effects on hippocampal neurons by using current- and voltage-clamp recordings in a hippocampal-slice preparation. Superfusion of cortistatin, like somatostatin-14, hyperpolarized these neurons (10 of 11 cells), in association with inhibition of action-potential firing (Fig. 4a), followed by recovery to control levels upon washout of the peptide. Unlike somatostatin, the cortistatin effect developed slowly, reaching a maximum 6–8 min after the onset of the response: somatostatin's effect on these neurons took 2–3 min to peak under the same conditions (not shown).

To determine the mechanism of this cortistatin-induced inhibition, we tested the effect of cortistatin on the M current (I_M), a non-inactivating voltage-dependent potassium current in hippocampal neurons⁷. Like somatostatin^{8,9}, cortistatin superfusion increased the amplitude of the I_M relaxation concomitantly with an outward steady-state current, with recovery to control levels upon washout (not shown).

The inhibition by cortistatin of excitability of CA1 pyramidal neurons was paralleled *in vivo* in the anaesthetized preparation. Field potentials were elicited in the CA1 region by stimulation of the commissural pathway. Stimulation of the monosynaptic afferent input to the CA1 region evoked a characteristic population spike (PS) that represents the synchronous firing of pyramidal cells, superimposed on a field synaptic potential waveform¹⁰. We generated stimulus–response curves to characterize the effects of cortistatin on extracellular recordings in CA1. Microiontophoretic application of cortistatin, like somatostatin, significantly decreased PS amplitudes both at half-maximal and maximal levels of stimulation (Fig. 4b).

As cortistatin is expressed in interneurons in the cerebral cortex and hippocampus, we investigated its effects on cortical measures of neuronal excitability. We infused up to 6 nmol HPLC-purified synthetic peptide into the brain ventricles of rats (n = 5) and recorded the electroencephalogram (EEG) for 4 hours after peptide injection. In addition, rats were observed for changes in spontaneous behaviour through a one-way window. Cortistatin-treated animals were clearly hypoactive compared with saline-injected rats, but kept their eyes open and displayed other signs of wakefulness for a short period (15–20 minutes). In these animals, the EEG showed a dramatic increase in cortical slow waves (1–4 Hz). Polygraphic monitoring of arousal states after cortistatin administration (Fig. 4c) also indicated that rats spent up to 75% of the 4-hour recording time in slow-wave sleep compared to 40%

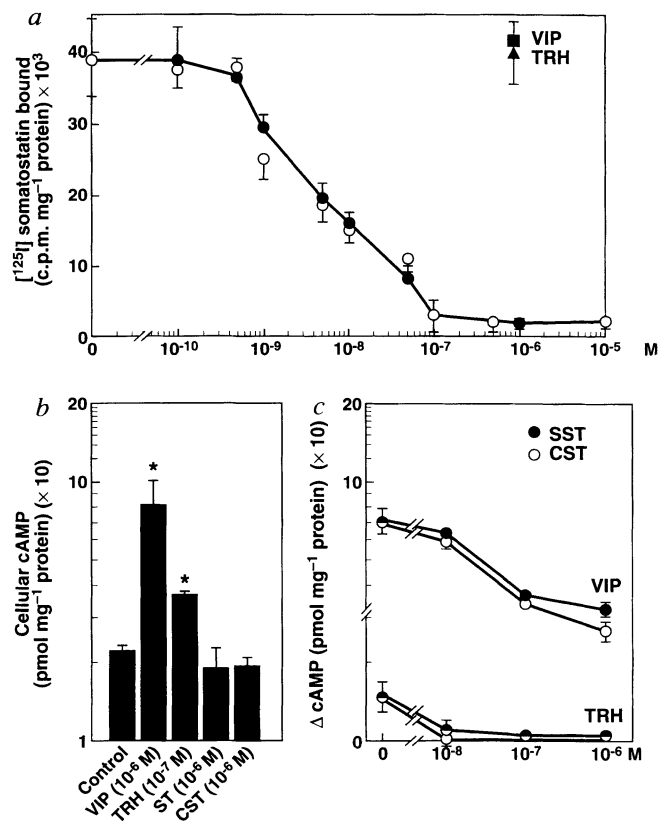
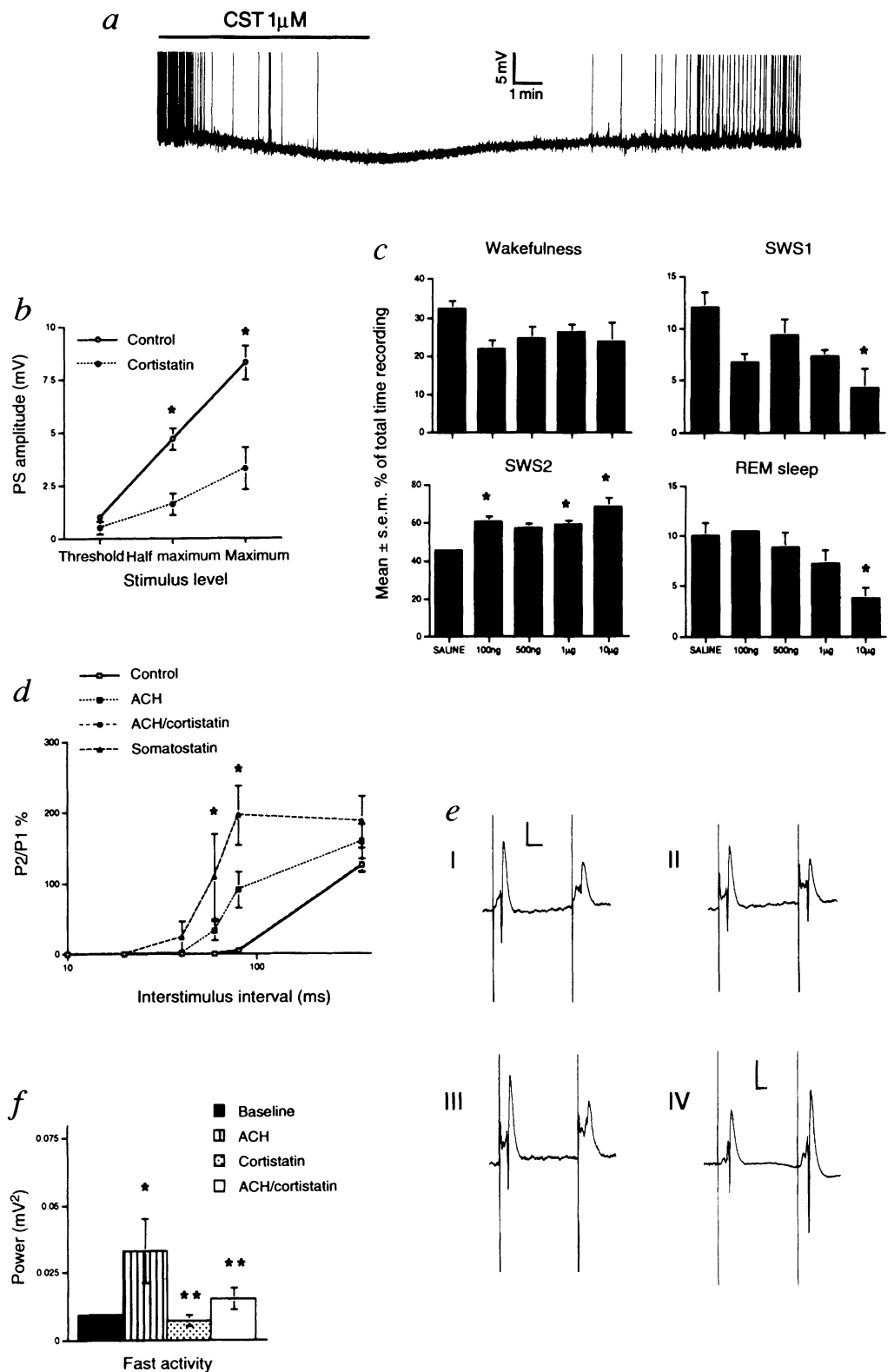


FIG. 3 Cortistatin binds to somatostatin receptors. **a**, Displacement by somatostatin and cortistatin of [¹²⁵I]-somatostatin bound to GH₄ pituitary cells. Cortistatin (filled circles) displaced [¹²⁵I]-somatostatin as effectively as somatostatin (white circles). The combined data from four independent experiments are plotted as mean ± s.e. TRH and VIP did not displace [¹²⁵I]-somatostatin. **b**, Cyclic AMP stimulation in GH₄ cells. Cultured cells were treated with VIP, TRH, somatostatin and cortistatin, and the intracellular cAMP was measured. VIP and TRH increased the intracellular concentration of cAMP whereas somatostatin or cortistatin did not. **c**, Inhibition of stimulated cAMP levels by somatostatin and cortistatin. Both statins were equally effective in inhibiting cAMP in VIP- or TRH-stimulated cells. METHODS. GH₄ cells were grown in MEM medium with 12% fetal calf serum in 6-well plates at 10⁶ cells ml⁻¹. Each well then received 10⁶ c.p.m. ml⁻¹ of [¹²⁵I]-somatostatin (NEN, DuPont), either alone or with increasing concentrations of somatostatin (Sigma), or cortistatin (95%; purified by reverse-phase HPLC). We included aprotinin and leupeptin (Sigma; 2 μg ml⁻¹), which reduced nonspecific binding to 20% of total bound radioactivity. We took the binding of [¹²⁵I]-somatostatin in the presence of 10⁻⁷ M somatostatin to represent nonspecific binding⁶. For cAMP experiments, we grew GH₄ cells under the same conditions as for binding experiments. Cells were washed with MEM without serum, but containing leupeptin, aprotinin and 1 mM 3-isobutylmethylxanthine. Cells were pretreated with somatostatin-14 (Sigma) and cortistatin-14 for 15 min and VIP (10⁻⁶ M; Bachem) or TRH (10⁻⁷ M; Calbiochem) was then added. [³H]-cAMP was added to each well before the content was removed, to calculate recovery. For cAMP measurements, we used a radioimmunoassay kit (Amersham) according to the manufacturer's instructions. Each time point represents 2–4 replicates; experiments were done twice.

for saline-treated control animals. We also observed a significant reduction in paradoxical (REM) sleep with the highest dose of cortistatin, in contrast to the reported increase in REM sleep after administration of a similar dose of somatostatin¹¹.

Because acetylcholine is a major regulator of sleep, we tested whether cortistatin produced its effects on sleep, in part, by altering cholinergic activity¹². We first examined the interactions between cortistatin and ACh on hippocampal CA1 neurons using evoked paired-pulse (PP) stimulation to test feed-forward and feedback inhibitory processes mediated in part by hippocampal

FIG. 4 Cortistatin modulates cortical and hippocampal electrophysiology *in vitro* and *in vivo*. **a**, Current-clamp recording of a CA1 neuron manually depolarized to -65 mV (resting membrane potential was -70 mV) to elicit action potential firing (upward deflections, truncated). Superfusion of $1 \mu\text{M}$ cortistatin-14 (bar above record) completely abolishes action potential discharge; the associated hyperpolarization is maximal at 7 min after onset of the response. **b**, Effects of cortistatin on population spike (PS) amplitudes in CA1 neurons *in vivo*. We generated stimulus-response curves and related the PS amplitude monotonically to stimulus intensity tested at three response levels: threshold, half-maximal and maximal (control mean half-maximal PS amplitude, 4.7 ± 0.5 mV; $n = 5$). Microiontophoretic application of cortistatin significantly decreased PS amplitudes in CA1. Asterisks represent significance levels at $P < 0.05$. **c**, Effect of intracerebroventricular administration of cortistatin on the sleep-wake cycle of the rat. Cortistatin increases the period of slow-wave sleep and decreases REM sleep. Asterisks, $P < 0.05$; ANOVA. **d**, Effects of iontophoretically applied ACh (0.9 M), somatostatin (1.5 mM) and cortistatin on PP responses in CA1 neurons *in vivo*. Stimulation intensity was adjusted after drug treatment to achieve control PS amplitudes before PP measurements were made (asterisks, $P < 0.05$). **e**, Representative recordings of field potentials elicited in CA1 by commissural stimulation. In the baseline recordings (I; calibration bars: 2 mV and 10 ms), the second response is completely inhibited at this interstimulus interval (80 ms). Iontophoretic administration of ACh reduced PP inhibition (II). This effect was antagonized by the simultaneous application of cortistatin (III). Somatostatin markedly decreased PP inhibition (IV; calibration bar, 1 mV and 10 ms). **f**, Effects of microiontophoretically (100 – 250 nA) applied ACh and cortistatin on local EEG activity recorded in the visual cortex. ACh markedly increased the averaged EEG power spectra (4-s epochs over 3 min) in the 8–16-Hz frequency band range. In contrast, the averaged EEG during infusion of cortistatin alone, or of ACh and cortistatin combined, did not differ from baseline. Results from the experimental groups were derived from averaged EEG spectral activity determinations and expressed as means \pm s.e.m. (asterisk, $P < 0.05$ from baseline; two asterisks, $P < 0.05$ from ACh; ANOVA). **METHODS**. Recordings were made intracellularly in rat hippocampal slices using sharp glass micropipettes¹⁹. We recorded from 11 hippocampal CA1 pyramidal cells with an average resting membrane potential of -70 ± 1 mV



(mean \pm s.e.m.) and action potential of 103 ± 2 mV. For the *in vivo* studies, male Sprague-Dawley rats were anaesthetized with halothane (0.9–1.1%). We stimulated the commissural pathway and elicited field potentials in the CA1 region as described¹⁵. Cortistatin (1 mg ml^{-1}) was dissolved in saline and administered iontophoretically through one barrel of a multibarrelled micropipette. We acquired data with software (LabView Instruments) as described¹⁵. Procedures for recordings and PP studies are described elsewhere^{20,21}.

Localization of dopamine D4 receptors in GABAergic neurons of the primate brain

L. Mrzljak*, C. Bergson†, M. Pappy*, R. Huff‡, R. Levenson† & P. S. Goldman-Rakic*

* Yale School of Medicine, Section of Neurobiology, 333 Cedar Street, New Haven, Connecticut 06510, USA

† Department of Pharmacology, Pennsylvania State University College of Medicine, Hershey, Pennsylvania 17033, USA

‡ Upjohn-Pharmacia Cell Biology, Kalamazoo, Michigan 49001, USA

interneurons^{13,14}. Half-maximal stimulation revealed a characteristic biphasic PP response curve¹⁵. Microiontophoretic application of ACh significantly antagonized the inhibitory phase of PP responses typical of interstimulus intervals of 60–80 ms ($P < 0.05$, Fig. 4d; data from 80-ms interval are shown in Fig. 4e, I–III). Cortistatin itself (not shown) had no significant effects on PP responses in CA1 but completely antagonized the effects of ACh ($P < 0.05$). The effects of somatostatin on PP responses were similar to those of ACh (Fig. 4d; data from 80 ms shown in Fig. 4e, IV). To determine whether cortistatin also interacts with cholinergic systems that regulate cortical function, we investigated the effects of cortistatin on ACh-induced desynchronization of EEG in the cerebral cortex of anaesthetized rats. Slow waves (0.5–4 Hz) dominated the EEG baseline of these rats, whereas iontophoretic administration of ACh desynchronized the local EEG by increasing the potency of the θ (4.5–8 Hz) and β (13–20 Hz) bands. This effect was prevented by simultaneous electrophoretic application of cortistatin (Fig. 4f).

We have described the isolation of a cDNA clone from an mRNA encoding the precursor of a new member of the somatostatin family whose distribution is primarily restricted to GABAergic cortical interneurons. Cortistatin-14 and somatostatin-14 appear to have similar inhibitory effects on the physiology of hippocampal neurons, suggesting that they could act through the same receptors *in vivo*. Cortistatin's effects on the activity of hippocampal neurons *in vivo* and on sleep physiology are, however, distinct from those of somatostatin, so cortistatin might bind differentially to different somatostatin-receptor subtypes from those analysed here, or it could act on μ -opioid receptors like the somatostatin analogue octeotride and the μ -receptor antagonist CTOP¹⁶. The different functional responses may indicate that there is an uncharacterized cortistatin receptor. The lack of effect of cortistatin on PP inhibition contrasts with the potent disinhibitory effect of somatostatin on this measure observed here, which is supported by somatostatin reduction of GABA-mediated synaptic potentials in CA1 pyramidal neurons¹⁷. This is another functional difference between cortistatin and somatostatin. These results are consistent with those from awake rats, in which cortistatin markedly reduces the duration of cortical electrical activity associated with the cholinergic system, as well as the ACh-induced desynchronization of local EEG. Therefore, cortistatin antagonizes the effects of ACh in both the hippocampus and the cerebral cortex *in vivo*. Our findings implicate this novel neuropeptide as a regulator of neuronal activity and sleep. □

DOPAMINE receptors are the principal targets of drugs used in the treatment of schizophrenia¹. Among the five mammalian dopamine-receptor subtypes, the D4 subtype is of particular interest because of its high affinity for the atypical neuroleptic clozapine^{1–3}. Interest in clozapine stems from its effectiveness in reducing positive and negative symptoms in acutely psychotic and treatment-resistant schizophrenic patients without eliciting extrapyramidal side effects⁴. We have produced a subtype-specific antibody against the D4 receptor and localized it within specific cellular elements and synaptic circuits of the central nervous system. The D4-receptor antibody labelled GABAergic neurons in the cerebral cortex, hippocampus, thalamic reticular nucleus, globus pallidus and the substantia nigra (pars reticulata). Labelling was also observed in a subset of cortical pyramidal cells. Our findings suggest that clozapine's beneficial effects in schizophrenia may be achieved, in part, through D4-mediated GABA modulation, possibly implicating disinhibition of excitatory transmission in intrinsic cortical, thalamocortical and extrapyramidal pathways.

Affinity-purified antibodies selectively bound to a protein of M_r ~40K which was present only in cell lines expressing the dopamine D4 receptor subtype, when examined by western blotting (Fig. 1a). Further, western blot analysis of a subcellular fractionation of the macaque hippocampus revealed D4 antibody reactivity with a ~41K protein present in synapsin-I-enriched membrane fractions (Fig. 1b). The M_r of proteins detected by the antibodies is in good agreement with the predicted size of the D4 receptor polypeptide (~42K)², strongly supporting the specificity of the antibodies for the D4 subtype of DA receptors.

In both the cerebral cortex and hippocampus, D4 receptor immunoreactivity was observed in pyramidal and in non-pyramidal neurons (Fig. 2a–d). These results are consistent with *in situ* hybridization evidence of D4 messenger RNA localization in the cerebral cortex⁵. The expression of D4 receptors in non-pyramidal neurons was notable because dopamine-receptor subtypes examined so far (D1 and D5) localize predominantly to pyramidal neurons both in cerebral cortex and hippocampus⁷. Most non-pyramidal neurons in the cerebral cortex are local circuit neurons or interneurons that release the inhibitory neurotransmitter GABA (γ -aminobutyric acid)⁸. Double-labelling with antibodies against GABA and/or the calcium-binding protein parvalbumin⁹ confirmed that the D4-positive non-pyramidal neurons were indeed GABAergic (Fig. 2e). In addition, electron microscopic analysis revealed asymmetric synapses on the cell bodies (Fig. 3a) and dendritic shafts (Fig. 3c) of the D4-labelled nonpyramidal neurons, a characteristic ultrastructural feature of interneurons. The immunoreaction product was frequently associated with the plasma membrane (Fig. 3a–c), endoplasmic reticulum and cytoplasm. It is not clear why the label associates with the cytoplasmic face of the plasma membrane, but this also occurs with antibodies to the predicted extracellular segments of other neurotransmitter receptors¹⁰. To our knowledge, the localization of D4 receptors in interneurons provides the first evidence of a role for this receptor in the modulation

Received 5 December 1995; accepted 21 March 1996.

- Shiromani, P. J., Gillin, J. C. & Henriksen, S. J. *Am. Rev. Pharmac. Toxicol.* **27**, 137–56 (1987).
- Borbely, A. A. & Tobler, I. *Physiol. Rev.* **69**, 605–670 (1989).
- Glushankov, P. et al. *Proc. natn. Acad. Sci. U.S.A.* **81**, 6662–6666 (1984).
- Veber, D. F. et al. *Nature* **280**, 512–514 (1979).
- Erlander, M. G. et al. *Neuron* **7**, 91–100 (1991).
- Schonbrunn, A. H. & Tashjian, A. J. R. *J. Biol. Chem.* **235**, 6473–6483 (1978).
- Halliwel, J. V. & Adams, P. R. *Brain Res.* **250**, 71–92 (1982).
- Moore, S. D. et al. *Science* **239**, 278–280 (1988).
- Schweitzer, P., Madamba, S. & Siggins, G. R. *Nature* **346**, 464–466 (1990).
- Andersen, P., Bliss, T. V. P. & Skrede, K. K. *Expl Brain Res.* **13**, 208–221 (1971).
- Danguir, J. *Brain Res.* **367**, 26–30 (1986).
- Steriade, M., McCormick, D. A. & Sejnowski, T. J. *Science* **262**, 679–685 (1993).
- Andersen, P., Eccles, J. C. & L oyning, Y. J. *Neurophysiol.* **27**, 607–619 (1964).
- Kandel, E. R. & Spencer, W. A. *J. Neurophysiol.* **24**, 243–259 (1961).
- Steffensen, S. & Henriksen, S. J. *Brain Res.* **538**, 46–53 (1991).
- Maurer, R. et al. *Proc. natn. Acad. Sci. U.S.A.* **79**, 4815–4817 (1982).
- Scharfman, H. E. & Schwartzkroin, P. A. *Brain Res.* **493**, 205–211 (1989).
- deLecea, L. et al. *Molec. Brain Res.* **25**, 286–296 (1994).
- Schweitzer, P. et al. *J. Neurosci.* **13**, 2033–2049 (1993).
- Prospero-Garcia, O., Criado, J. R. & Henriksen, S. J. *Pharmac. Biochem. Behav.* **49**, 413 (1994).
- Steffensen, S. C., Campbell, I. L. & Henriksen, S. J. *Brain Res.* **652**, 149 (1994).

ACKNOWLEDGEMENTS. We thank F. E. Bloom, F. H. Burton, M. Morales, P. Ruiz-Lozano and P. P. Sanna for helpful comments and A. Tobin for rat GAD65 and 67 plasmids. K.M.G. was on sabbatical leave from the University of Oslo. This work was supported in part by grants from NINDS, NIGM, NIDA and NIMH to G.R.S., S.J.H. and J.G.S.

CORRESPONDENCE and requests for materials should be addressed to J.G.S. The accession number for precortistatin cDNA sequence is U51919.